Analysis of the Thermal Absorption by Flash Fusible Toner

*Teruaki Mitsuya**
Hitachi Research Laboratory, Hitachi, Ltd., Hitachi, Ibaraki 319-12, Japan

Melany L. Hunt
Division of Engineering and Applied Sciences, California Institute of Technology, Pasadena, California 91125

Abstract

A toner particle is composed of submicrometer carbon black particles that are suspended in a polymeric resin. In flash fusing, the energy distribution has a broad wavelength distribution. Therefore the variation of the effective complex refractive indices with wavelength is required to determine the absorption coefficient. An approximation, performed by means of Maxwell Garnett theory, is used to estimate the indices. The spectral geometric optics approach is employed to determine the internal distribution of radiant absorption. The results indicate that the absorbed energy increases dramatically near 2 wt% carbon black content. In the region beyond the sharp increase, the absorbed energy plateaus. In the range of the sharp increase, considerable energy penetrates to the back of the particle. For the higher carbon weight ratios, most of the energy is absorbed just below the irradiated surface. For less than 2.5 wt%, the absorbed energy seems to be uniformly distributed. For fixing a toner particle, a large temperature increase at the interface between the toner particle and the paper is required. From this point of view, both uniformity and high percentage absorbed energy are desired. Both requirements can be satisfied by carbon content near 2.5 wt%, which is proposed as the optimum value.

Introduction

In the fixing process in electrophotographic machines, toner is heated above the glass transition temperature and fused to the substrate paper. The two common types of fixing processes, which use either radiant or conductive heating, are called flash fusing[1,2] and heat roll fusing,[3,4] respectively. Flash fusing, for which a xenon flash lamp is used, has the advantage of stable paper handling in high-speed printing, owing to minimal paper strain during heating. The paper is not heated significantly, because most of the flash wavelengths are in the visible region and are reflected. The radiant energy may be absorbed only at the surface of the toner layer, which may result in a significant temperature distribution through the toner. If the interface temperature between the toner and the paper is not large enough, the toner may not properly adhere to the paper.

Previous studies have analyzed the temperature field in the toner layer during flash fusing.[1,2] However, surface-concentrated radiant absorption has been assumed. The temperature field during fusing may be affected by the internal distribution of radiant absorption in the toner particle, which has not been investigated in previous studies. A method developed for estimating the internal distribution of radiant absorption in a toner particle irradiated by a flash lamp is presented here.

Electrophotographic Process and Flash Fusible Toner

The electrophotographic process is widely used in copy machines and laser printers. The process is shown in Fig. 1. At first, a photoconductor drum is electrically charged uniformly, and then the charge is partly erased by applying a light image. This exposure builds up a latent image of electric charge. Next, the developing device places charged toner on the drum surface that holds the latent image, and the toner image is transferred to a paper surface. After that, the toner is fused on the paper by the fuser to produce the final fixed toner image.

Fixing, which is the final process in an electrophotographic machine, determines print qualities such as fixing strength and glossiness of the image. Figure 2 shows a measured result in arbitrary units of a typical spectroscopic relative energy distribution of a xenon flash. The electric power supply is set at 1.6 J/cm^2. In this condition the measured radiant energy from the lamp is 0.43 J/cm^2. Normally the electric power supply is set in a range of 1.4-2.0 J/cm^2. The distribution is variable with the area density of electric current and the xenon gas pressure in the lamp. The energy distribution has a wide spectrum, which includes the visible region.

The flash fusible toner is composed mainly of epoxy or styrene-acrylic resins. Normally, 5-10 wt% of carbon black powder, with an average particle diameter near 100 nm, is added for black coloring. In addition, a small amount of charge control agent is included for the developing process. The diameter of toner particles varies in a range of 5-20 μm. Its mean diameter is measured as 9.6 μm. The carbon black plays a significant role, not only as a black

coloring pigment, but also as a radiant energy absorber. Therefore the optimized carbon black content should be a significant item in the design of the flash fusible toner. In this study, the toner material is assumed to be composed of the epoxy resin and the carbon black (graphite), and the toner particle is assumed to be spherical and to be 9.6 μm in diameter.

Before calculating the absorption, it is necessary to estimate the scattering effect. The energy scattered by the carbon black particle embedded in the epoxy resin is calculated by Mie theory.[5] Figure 2 shows the portion of the incident energy that is scattered by the carbon black particles. Compared with the total incident energy, the scattered energy is small. Furthermore, because the clearance between the particles is very small (220 nm at 2 wt% of carbon black, 80 nm at 10 wt%), the scattered energy may be secondarily absorbed by neighboring particles located very closely. Therefore the effect of the scattering is negligible and is not considered in this study.

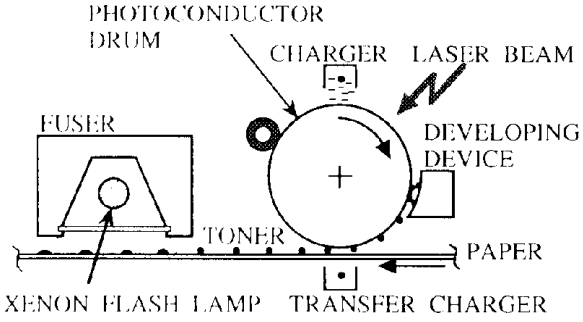

Figure 1. Electrophotographic process.

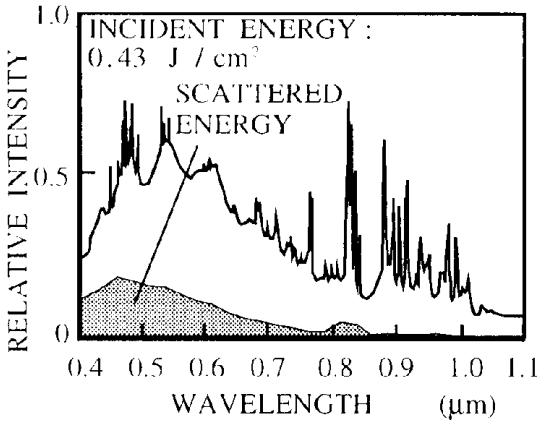

Figure 2. Flash energy distribution.

The effective complex refractive indices are required to determine the absorption coefficient, which is needed to calculate the radiant energy absorption. An approximation, calculated by means of Maxwell Garnett theory,[5,6] is employed to estimate the indices.

Application of Maxwell Garnett Theory

Maxwell Garnett Theory

The toner material contains particles of carbon black that are smaller in diameter than the wavelength of the incident light. For this type of amorphous material, Maxwell Garnett theory works well.[5,6] The effective complex refractive index, *Ne, is* derived from Eq. 1,

$$Ne(\lambda_0)^2 = \frac{1+2pf(\lambda)}{1-pf(\lambda)} \cdot Na(\lambda)^2, \quad (1)$$

where *Na,* λ, and λ_0 are the complex refractive index of the matrix, the wavelength of the light in the matrix material, and the incident light, respectively, and *f is* defined in Eq. 2,

$$f(\lambda) = \frac{Nf(\lambda)^2 - Na(\lambda)^2}{Nf(\lambda)^2 + 2Na(\lambda)^2}. \quad (2)$$

The term *Nf is* the complex refractive index of the inclusions. In Eq. 1 *p* is the volume fraction of the inclusions, which can be calculated from the following equation,

$$p = \frac{\gamma_r \cdot R}{\gamma_r \cdot R + \gamma_c (1-R)}, \quad (3)$$

where *R,* γ_c, and γ_r are shown as the weight ratio of the carbon black, the specific weight of the carbon black material (graphite), and the epoxy resin, respectively. The complex refractive index of the resin has only a real part, which varies from 1.5 to 1.7 over the wavelength range of interest. Therefore the real number of 1.6 is employed for *Na.* The complex refractive index of the carbon black inclusion contains real and imaginary parts and varies with the wavelength. The values of *Nf*(λ) are derived from the published values of the complex electric permittivity.[5,8] The calculated value of *Nf*(λ) varies in the ranges 1.20–2.58 for the real part and 1.38–2.30 for the imaginary part.

Calculated Optical Properties of Toner Material

Figure 3 shows the effective complex-refractive indices of toner material derived by Eqs. 1-3. For the higher carbon weight ratios, the values of *n* and *k* are higher and increase more dramatically at lower wavelengths than do the values for lower carbon weight ratios.

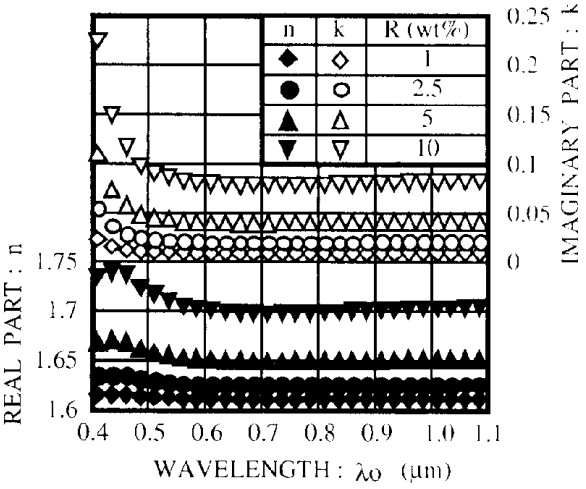

Figure 3. Complex refractive index.

Bruggeman theory is also a well-known method to estimate the effective optical properties.[5] The effective com-

plex refractive indices of toner material are derived by Bruggeman theory to confirm the accuracy of the approximation. The results from Maxwell Garnett and Bruggeman theories correspond within 3% over most of the range and within 10% for low wavelengths.

The effective absorption coefficient, *a,* of the toner material can be calculated by substituting *n* and *k* in Eq. 4.

$$a(\lambda_0) = \frac{4\pi \cdot n(\lambda_0)}{\lambda_0} \cdot k(\lambda_0). \tag{4}$$

Figure 4 shows the effective absorption coefficient of the toner material derived by Eq. 4. In the lower range of λ_0, the absorption coefficient is significantly larger than in the infrared range, reflecting the changes in *k.* Because of significant variation of the effective absorption coefficient, a spectral analysis is used for the radiant absorption distribution.

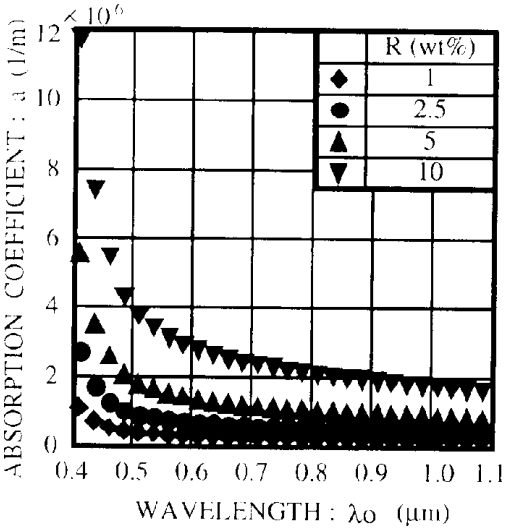

Figure 4. Absorption coefficient.

Evaluations of the Absorption

Method to Calculate Absorption

The geometric optics approach is used to determine the internal distribution of radiant absorption in the toner particle. The paper of Tuntomo, Tien, and Park[7] indicates a negligible difference between the electromagnetic theory and the geometric optics approach if the size parameter, $\pi d/\lambda_0$, is greater than 10, where *d* is the particle diameter. Because the size parameter for the toner particles over the wavelength range of interest is greater than 14, each method can be applicable.

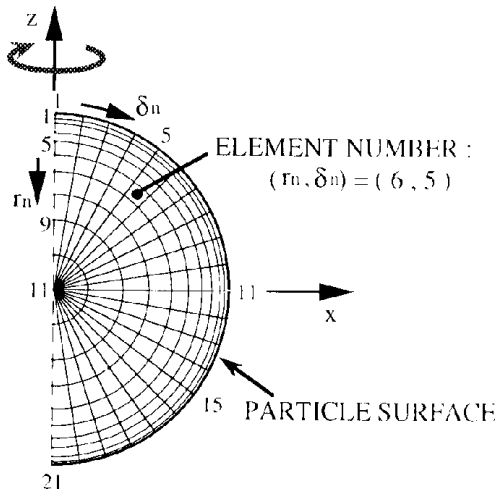

Figure 5. Coordinates.

Figure 5 shows the coordinates for the estimation. An axisymmetric coordinate for the z axis is employed. The incident flash irradiates the toner particle from the z direction. To determine the absorption distribution, the particle is divided into 200 elements. Figure 6 shows the ray path. Each internal ray path differs with the location and with the wavelength of the incident flash ray. Hence, for a location, *i*, and a wavelength, *j*, the ray path can be shown as Eq. 5

$$\sin\theta(i,j) = \frac{1}{n(j)} \cdot \sin\theta_0(i). \tag{5}$$

By denoting the spectroscopic intensity shown in Fig. 2 as i_0, the total intensity over the range of spectrum of the ray across a certain area as I_0, and expressing the total irradiated energy of the flash as *Q*, the energy entering into the particle for the ray (*i, j*), *q*(*i, j*), is determined from

$$q(i,j) = Q \cdot \frac{i_0(i,j)}{I_0(i)} \cdot (1-\rho(i,j)), \tag{6}$$

where ρ(*i, j*) is the spectral reflectance of the ray (*i, j*) and is calculated as

$$\rho(i,j) = \frac{1}{2}\left[\frac{(n(j)\cdot\cos\theta_0(i) - u(i,j))^2 + v(i,j)^2}{(n(j)\cdot\cos\theta_0(i) + u(i,j))^2 + v(i,j)^2} + \frac{(n(j)^2\cdot(1-k(j)^2)\cdot\cos\theta_0(i) - u(i,j))^2 + (2n(j)^2\cdot k(j)\cdot\cos\theta_0(i) - v(i,j)^2}{(n(j)^2\cdot(1-k(j)^2)\cdot\cos\theta_0(i) + u(i,j))^2 + (2n(j)^2\cdot k(j)\cdot\cos\theta_0(i) + v(i,j)^2}\right] \tag{7}$$

and

$$u(i,j) = \sqrt{\tfrac{1}{2}[n(j)^2\cdot(1-k(j)^2) - \sin^2\theta_0(i) + \sqrt{(n(j)^2\cdot(1-k(j)^2) - \sin^2\theta_0(i))^2 + 4n(j)^4 k(j)^2}\,]} \tag{8}$$

$$v(i,j) = \sqrt{\tfrac{1}{2}[-n(j)^2\cdot(1-k(j)^2) + \sin^2\theta_0(i) + \sqrt{(n(j)^2\cdot(1-k(j)^2) - \sin^2\theta_0(i))^2 + 4n(j)^4 k(j)^2}\,]}. \tag{9}$$

The energy per unit volume, *Ea*, that is locally absorbed in the element (r_n, δ_n) is calculated from the summation of the energy absorbed by every ray that crosses it and is shown as

$$Ea(r_n,\delta_n) = \frac{1}{V(r_n,\delta_n)}\cdot\sum_N [q(i,j)\cdot\{\exp(-a(j)\cdot l_{r_n,\delta_n}(i,j)) - \exp(-a(j)\cdot(l_{r_n,\delta_n}(i,j)+\Delta l_{r_n,\delta_n}(i,j)))\}], \quad (10)$$

where $V(r_n, \delta_n)$ is the volume of the element and subscript n is the number of rays that cross the element.

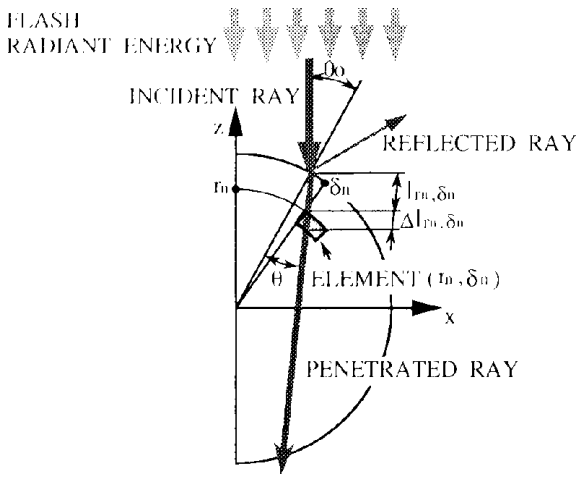

Figure 6. Ray path.

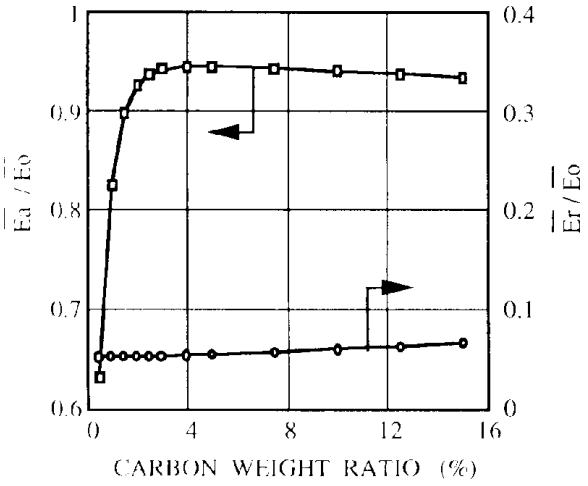

Figure 7. Total Energy

Radiant Absorption Distributions

Figure 7 shows the total absorbed and reflected energy, $\overline{Ea}$ and $\overline{Er}$, for toner particles with various amounts of carbon black. Their values are the spectral averages of the results for each element calculated by the above equations. The vertical axis is normalized by the value of the total incident energy, $\overline{Er}$ (= *Q*). The absorbed energy increases dramatically near 2 wt% carbon black content. In the region beyond the sharp increase, $\overline{Ea}$ plateaus and then gradually decreases, corresponding with the gradual increase of the reflected energy, $\overline{Er}$. In the range of the sharp increase, the sum of $\overline{Ea}/\overline{Eo}$ and $\overline{Er}/\overline{Eo}$ is less than 1, indicating that considerable energy penetrates to the back of the particle. The radiant absorption distributions, with the carbon black content, are shown in Figures 8(a) to 8(d). Figure 8(a) is for 1 wt% carbon black and is in the sharply increasing region of $\overline{Ea}$, which is observed in Figure 7. Figure 8(b) is for 2.5 wt% carbon black and corresponds with the beginning of the plateau region of absorption. Figures 8(c) and 8(d)are for two higher values of carbon black content, 5 and 10 wt%. For the higher carbon weight ratios, most of the energy is absorbed just below the irradiated surface. For less than *2.5* wt%, the absorbed energy appears to be uniformly distributed through the particle. At 1 wt%, the absorption at the back surface of the toner is remarkably high, which results from a focusing of the ray path toward the interior by the surface refraction.

The adhesion between the toner and the paper is improved by increasing the temperature at the back surface of the toner.[1,4] From this point of view, uniform absorption distribution is desired. However, if the carbon black content is too low, the total absorbed energy may be low, as shown in Figure 7. Therefore, for an optimum carbon weight ratio, the value of the carbon content should be slightly beyond the sharp increase, so that the requirements of uniform heating and high absorptivity can be satisfied. The optimum range might be further clarified by a thermal conduction analysis in the spherical particle, in which the results of the absorption shown in Figure 8 are used to calculate the input energy.

Conclusions

The radiant absorption distributions in the flash fusible toner particle are examined to guide toner design.

1. In the lower wavelength range of the incident light, the value of the imaginary part in effective complex refractive index of the toner material increases significantly. As a result, the effective absorption coefficient changes in a similar manner, requiring a spectral analysis to study the radiation problem for flash fusible toner particles.
2. The absorbed energy increases sharply with an increase of carbon black content near 2 wt%. At the beginning of the plateau, near 2.5 wt%, 94% of the incident energy is absorbed in the particle, and the absorption is uniformly distributed. For higher carbon weight ratio, the total absorption increases slightly to 95%, but the absorption is concentrated toward the front of the particle.
3. A large temperature increase at the interface between the toner particle and the paper is required for fixing. From this point of view, both uniformity and a high percentage of absorbed energy are desired. Both requirements can be satisfied by carbon content near 2.5 wt%, which is proposed as the optimum value.

Acknowledgment

The present work was carried out at the California Institute of Technology with the head author on leave from Hitachi

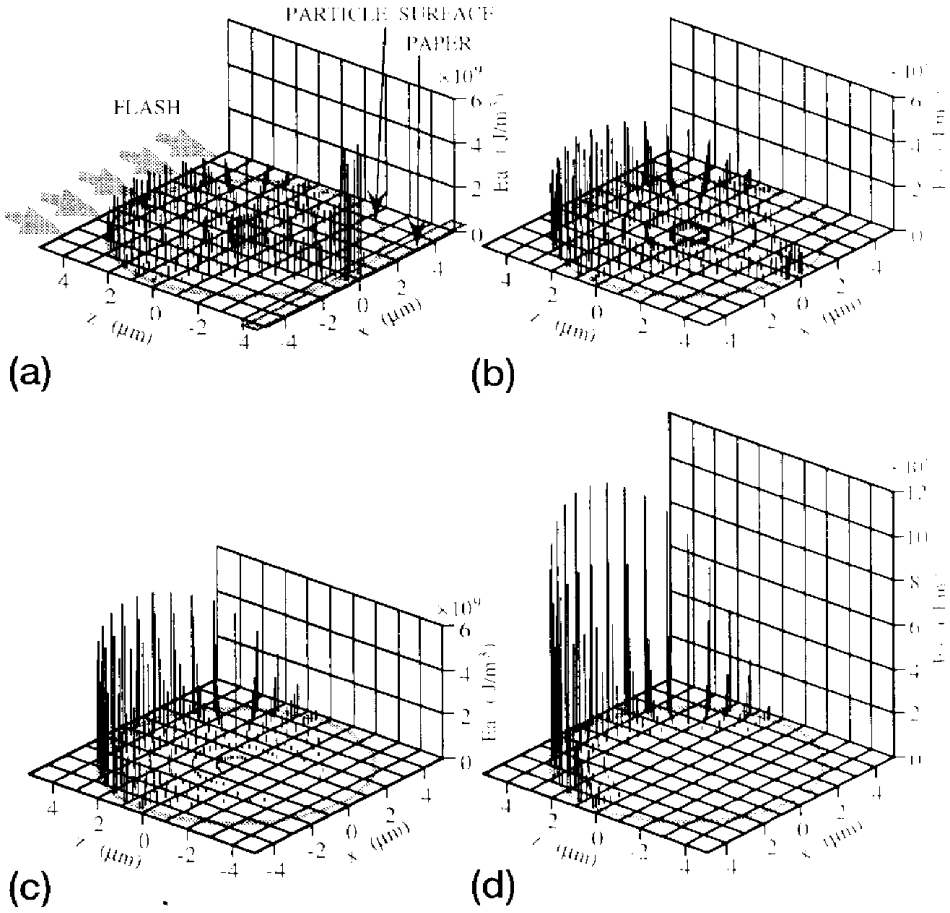

Figure 8. Distributions of local absorbed energy (a) Carbon weight ratio, 1%, (b) carbon weight ratio, 2.5%; (c) carbon weight ratio, 5%; (d) carbon weight ratio, 10%.

Research Laboratory, Hitachi, Ltd. The authors wish to express their appreciation to Hitachi, Ltd., for its sponsorship.

References

1. T. Mitsuya, T. Kumasaka, and S. Fujiwara, Study of temperature and toner melting conditions during flash fusing, *Optical Engineering* **30**: 111-116 (1991).
2. H. S. Kocher, Study of heat transfer in toner during flash fusing by means of electrical analog networks, *IEEE Industry Applications Society Conference Record,* 1979 pp. 3442.
3. T. Mitsuya, and T. Kumasaka, Heat transfer and toner meting in an electrophotographic fuser system, *J. Imaging Sci. Technol.* **36**: 88-92 (1992).
4. T. Mitsuya, K. Masuda, and Y. Hori, Measurement of temperature and heat flux changes during fixing process in electrophotographic machines, *1992 ASME winter Annual Meeting*, *Pamphlet Paper 92- WA/DE-* U *2,* 1992.
5. C. F. Bohren, and D. R. Huffman, Absorption and scattering of light by small particles, John Wiley & Sons, New York, 1983, pp. 181-267.
6. J. C. Maxwell Garnett, Colours in metal glasses in metallic films, *Phil. Trans. Royal Soc*., **203**: 385420 (1904).
7. A Tuntomo, C. L Tien, and S. H. Park, Internal distribution of radiant absorption in a spherical particle, *J. Heat Transfer* **113**: 407-412 (1991).
8. D. R. Huffman, Interstellar grains: the interacton of light with a small-particle system, *Adv. Phys.* **26**: 129-230 (1977).